The 2013 World Congress on
Advances in Structural Engineering and Mechanics (ASEM13)
Jeju, Korea, September 8-12, 2013

Wave Induced Motion of a Triangular Tension Leg Platforms in Deep Waters

*A. M. Abou-Rayan [1)], and Amr R. El-gamal [2)]

[1)] *Civil Engineering Department, Northern Border Univ., KSA.*
[2)] *Civil Engineering Technology Department, Benha Univ., Egypt.*

ABSTRACT

Tension leg platforms (TLP's) are highly nonlinear due to large structural displacements and fluid motion-structure interaction. Therefore, the nonlinear dynamic response of TLP's under hydrodynamic wave loading is necessary to determine their deformations and dynamic characteristics. In this paper, a numerical study using modified Morison Equation was carried out in the time domain to investigate the influence of nonlinearities due to hydrodynamic forces and the coupling effect between all degrees of freedom on the dynamic behavior of a TLP. The stiffness of the TLP was derived from a combination of hydrostatic restoring forces and restoring forces due to cables and the nonlinear equations of motion were solved utilizing Newmark's beta integration scheme. The effect of wave characteristics was considered.

1. INTRODUCTION

The TLP can be modeled as a rigid body with six degrees of freedom (6-DOF), which can be conveniently divided into two categories, those controlled by the stiffness of tethers, and those controlled by the buoyancy. The former category includes motion in the vertical plane and consists of heave, roll and pitch; whereas the latter comprises the horizontal motions of surge, sway and yaw .The natural periods of motion in the horizontal plane are high, whereas in the vertical plane the periods are low. Generally, the surge and sway motions are predominantly high for head seas due to the combined actions of wind, waves and currents. However, due to coupling among various degrees of freedom and relatively low damping of hydrodynamic origin in the vertical plane motion, a complete analysis of a 6-DOF system subjected to wind, waves and currents is desirable. Moreover**,** the structural flexibility in the horizontal motions causes nonlinearity in the structural stiffness matrix because of large deformations.

The natural periods of the horizontal plane motions are higher than typical wave period which precludes resonance with the wave diffraction forces. However, the wave-induced low frequency forces, namely the wave drift forces, could be close to the natural periods of motion in the horizontal plane causing a significant response of a TLP despite the low amplitude of these forces. The maximum TLP response at low frequencies in various extreme environmental conditions is of primary importance from

---

* Corresponding Author, Associate Prof., Ph.D., Email: aabourayan@yahoo.com

the point of view of platform stability, serviceability and fatigue of tethers.

A number of studies have been conducted on the dynamic behavior of TLP's under both regular and random waves. Chandrasekaran and Roy (2005), presented phase space studies of offshore structures subjected to nonlinear dynamic loading through Poincare maps for certain hydrodynamic parameters. Bhattachatya et al. (2004) investigated coupled dynamic behavior of a mini TLP giving special attention to hull-tether coupling. Ketabdari and Ardakani (2005) developed a computer program to evaluate the dynamic response of sea-star TLP to regular wave forces considering coupling between different degrees of freedom. Lee and Wang (2000) investigated the dynamic behavior of a TLP with a net-cage system with a simplified two-dimensional modeling. Low (2009) presented a formulation for the linearization of the tendon restoring forces of a TLP. Chandrasekaran et al. (2007a) conducted dynamic analysis of triangular TLP models at different water depths under the combined action of regular waves and an impulse load affecting the TLP column. Chandrasekaran et al. (2007b) focused on the response analysis of triangular TLP for different wave approach angles. Kurian et al. (2008a and 2008b) developed a numerical study on determining the dynamic responses of square and triangular TLPs subjected to random waves. Yang and Kim (2010) developed a numerical study of the transient effect of tendon disconnection on the global performance of an extended tension leg platform (ETLP) during harsh environmental conditions of the gulf of Mexico. Recently, Abou-Rayan et.al, (2012), have investigated the dynamic response of a square TLP under hydrodynamic forces in the surge direction considering all degrees of freedom of the system. They developed a numerical dynamic model for the TLP where Morison's equation with water particle kinematics using Airy's linear wave theory was used.

In this paper, a numerical study was conducted to investigate the dynamic response of a triangular TLP (shown in Fig. 1) under hydrodynamic forces considering all degrees of freedom of the system. The analysis was carried out using modified Morison equation in the time domain with water particle kinematics using Airy's linear wave theory. The influence of nonlinearities due to hydrodynamic forces and the coupling effect between surge, sway, heave, roll, pitch and yaw degrees of freedom on the dynamic behavior of TLP's was investigated. The stiffness of the TLP was derived from a combination of hydrostatic restoring forces and restoring forces due to cables and the nonlinear equations of motion were solved utilizing Newmark's beta integration scheme. The effect of wave characteristics such as wave period and wave height on the response of TLP's was evaluated. Only uni-directional waves in the surge direction was considered in the analysis.

2. STRUCTURAL IDEALIZATION AND ASSUMPTIONS

The general equation. of motion of the TLP model under a regular wave is given as

$$[M]\{x^{\bullet\bullet}\}+[C]\{x^{\bullet}\}+[K]\{x\}=\{F(t)\} \tag{1}$$

Where, $\{x\}$ is the structural displacement vector, $\{\dot{x}\}$ is the structural velocity vector, $\{\ddot{x}\}$ is the structural acceleration vector; $[M]$ is the structure mass matrix; $[C]$ is the structure damping matrix; $[K]$ is the structure stiffness matrix; and $\{F(t)\}$ is the

hydrodynamic force vector. The mathematical model derived in this study assumes that the platform and the tethers are treated as a single system and the analysis is carried out for the 6-DOF under different environmental loads where wave forces are estimated at the instantaneous equilibrium position of the platform utilizing Morison's equation and using Airy's linear wave theory. Wave force coefficients, C_d and C_m, are the same for the pontoons and the columns and are independent of frequencies.

3. DEVELOPMENT OF A TRIANGULAR TLP MODEL

3.1. Draft evaluation

At the original equilibrium position, Fig. 1, summation of forces in the vertical direction gives:

$$W + T = F_B \tag{2}$$

So,

$$W + (3T_o) = F_B \tag{3}$$

$$F_B = \frac{3}{4}\rho\pi g(D_c^2 D_r + D_p^2 s) \tag{4}$$

From Eq.(4) , we find that

$$D_r = \left[[\{(W + T)/(\frac{3}{4}\rho\pi g) - (D_p^2 s)]/ D_c^2 \right] \tag{5}$$

where, F_B is the total buoyancy force; W is the total weight of the platform in air; T is the total instantaneous tension in the tethers; T_o is the initial pre-tension in the tether; ρ is the mass density of sea water; D_c is the diameter of TLP columns; D_p is the diameter of pontoon; S is the length of the pontoon between the inner edges of the columns and D_r is the draft.

3.2. Stiffness matrix of Triangular TLP configuration

The stiffness of the platform is derived from a combination of hydrostatic restoring forces and restoring forces due to cables. Restoring force for motions in the horizontal plane (surge, sway, and yaw) are the horizontal component of the pretension in cables, while restoring forces for motions in the vertical plane arise primarily from the elastic properties of cables, with a relatively small contribution due to hydrostatic forces. The coefficients, *Kij*, of the stiffness matrix of the triangular TLP are derived from the first principles as the reaction in the degree of freedom *i,* due to unit displacement in the degree of freedom *j*, keeping all other degrees of freedom restrained. Moreover, the tether tension changes due to the motion of the TLP in different degrees of freedom leads to a response-dependent stiffness matrix. The coefficients of the stiffness matrix [*K*] of a triangular TLP are

$$[K]=\begin{pmatrix} K_{11} & 0 & 0 & 0 & K_{15} & 0 \\ 0 & K_{22} & 0 & K_{24} & 0 & 0 \\ K_{31} & K_{32} & K_{33} & K_{34} & K_{35} & K_{36} \\ 0 & K_{42} & 0 & K_{44} & 0 & 0 \\ K_{51} & 0 & 0 & 0 & K_{55} & 0 \\ 0 & 0 & 0 & 0 & 0 & K_{66} \end{pmatrix} \tag{6}$$

and can be determined as following

Surge (1) direction The coefficients of the first column of the restoring force matrix are found by giving a unity x displacement in the x-direction (surge) as shown in Fig. 2. The increase in the initial pre-tension in each leg is given by

$$\Delta T_1 = \frac{E \times A \times \Delta L}{L} \quad , \qquad \Delta L = \sqrt{x_1^2 + L^2} - L \tag{7}$$

where A is the cross-sectional area of the tether; E is the Young's Modulus of the tether; ΔT_1 is the increase in the initial pre-tension due to the arbitrary displacement given in the surge degree of freedom; L is the length of the tether; and x_1 is the arbitrary displacement in the surge degree of freedom. Equilibrium of forces in different directions gives

$$K_{11} = \frac{3(T_o + \Delta T_1)}{\sqrt{x_1^2 + L^2}} \tag{8}$$

$$K_{31} = \left[3T_o \left(\frac{L}{\sqrt{x_1^2 + L^2}} - 1 \right) + 3\Delta T_1 \frac{L}{\sqrt{x_1^2 + L^2}} \right] \Big/ x_1 \tag{9}$$

$$\sum Mx = O = K_{41}\, x_1 \Rightarrow K_{41} = O \tag{10}$$

$$K_{51} = (-K_{11}\, h) \ , \ \sum Mz = O = K_{61}\, x_1 \Rightarrow K_{61} = O \tag{11}$$

Sway (2) direction The coefficients of the second column of the restoring force matrix are found in a similar manner by as shown in Fig. 3.

$$K_{12} = 0,\ K_{52} = 0 \ \text{ and } \ K_{62} = 0 \tag{12}$$

$$K_{22} = \frac{3(T_o + \Delta T_2)}{\sqrt{x_2^2 + L^2}} \tag{13}$$

$$K_{32} = \left[3T_o \left(\frac{L}{\sqrt{x_2^2 + L^2}} - 1 \right) + 3\Delta T_2 \frac{L}{\sqrt{x_2^2 + L^2}} \right] \Big/ x_2 \tag{14}$$

$$K_{42} = -h K_{22} \tag{15}$$

Where ΔT_2 is the increase in tension due to sway and is given by

$$\Delta T_2 = \frac{E \times A \times \Delta L}{L} \quad , \qquad \Delta L = \sqrt{x_2^2 + L^2} - L \tag{16}$$

Note that δ_x and δ_y shown in Fig.s 2 and 3 are the angles of inclination of the cables with respect to the vertical when under surge and sway movements, respectively.

Heave (3) direction The third column is derived by giving the structure an arbitrary displacement in the z direction (heave). The sum of the forces in the all directions yield

$$K_{13} = K_{23} = K_{43} = K_{53} = K_{63} = 0 \quad , \quad k_{33} = 3\frac{EA}{L} + 3\frac{\pi D_c^2}{4}\rho g \tag{17}$$

Roll (4) direction The coefficients in the fourth column of the restoring force matrix are found by giving the structure in arbitrary rotation x_4 about the x-axis as shown in Fig. 4. Summation of the moments of the resulting forces about the x-axis yields

$$K_{14} = K_{54} = K_{64} = 0 \tag{18}$$

Taking summation of forces in y-axis and z-axis, respectively we find that

$$k_{24} = \frac{\left[((T_o + \Delta T_{14})Sin\theta_{14} + (T_o + \Delta T_{04})Sin\theta_{04} + (T_o + \Delta T_{24})Sin\theta_{24})\right]}{x_4} \tag{19}$$

$$k_{34} = \frac{(T_o + \Delta T_{14})Cos\theta_{14} + (T_o + \Delta T_{04})Cos\theta_{04} + (T_o + \Delta T_{24})Cos\theta_{24} - 3T_o}{x_4} \tag{20}$$

and taking summation of moments about x axis we get

$$k_{44} = \left[\begin{array}{l} ((T_o + \Delta T_{14})Cos\theta_{14}(\frac{PL}{2} + e_{14}) + (T_o + \Delta T_{04})Cos\theta_{04} \times e_{04} \\ -(T_o + \Delta T_{24})Cos\theta_{24}(\frac{PL}{2} - e_{24)}) + F_B \times e_{o4} + (T_o + \Delta T_{14})Sin\theta_{14}(H - h_{14}) \\ +(T_o + \Delta T_{04})Sin\theta_{04} \times (H - h_{04}) + (T_o + \Delta T_{24})Sin\theta_{24}(H - h_{24)}) \end{array}\right] \Big/ x_4 \tag{21}$$

Pitch (5) direction The coefficients in the fifth column of the restoring force matrix are found by giving the structure an arbitrary rotation x_5 about the y-axis (see Fig. 6). Summation of the moments of the resulting forces about the y-axis gives

$$K_{25} = K_{45} = K_{65} = 0 \tag{22}$$

By taking summation of forces in the x-, z-directions, and moments about y-axis respectively, we find that

$$k_{15} = \frac{\left[(2(T_o + \Delta T_{15})Sin\theta_{15} + (T_o + \Delta T_{25})Sin\theta_{25})\right]}{x_5} \tag{23}$$

$$k_{35} = \frac{\left[2(T_o + \Delta T_{15})Cos\theta_{15} + (T_o + \Delta T_{25})Cos\theta_{25} - 3T_o\right]}{x_5} \tag{24}$$

$$k_{55} = \left[\begin{array}{l} 2(T_o + \Delta T_{15})Cos\theta_{15}(\frac{Pb}{3} + e_{15}) - (T_o + \Delta T_{25})Cos\theta_{25}(\frac{2Pb}{3} - e_{25}) \\ + F_B \times e_{o5} + (T_o + \Delta T_{25})Sin\theta_{25}(H - h_{25}) + (T_o + \Delta T_{15})Sin\theta_{15} \times (H - h_{15})) \end{array}\right] \Big/ x_5 \tag{25}$$

Yaw (6) direction By giving an arbitrary rotation x_6 in the yaw degree of freedom, the sixth column of the restoring force matrix can be obtained (see Fig. 7). We can find that

$$K_{16} = K_{26} = K_{46} = K_{56} = 0 \tag{26}$$

By taking summation of moment about z-axis and summation of forces in the vertical direction one obtains

$$K_{66} = 3(T_o + \Delta T_6)\frac{(2a^2)}{L_1} \quad , \quad K_{36} = [3T_o(\frac{L}{L_1} - 1) + 3\Delta T_6(\frac{L}{L_1})]/x_6 \tag{27}$$

The overall stiffness matrix given by Eq.(6) shows

1. The presence of off-diagonal terms, which reflects the coupling effect between the various degrees of freedom.
2. The coefficients depend on the change in the tension of the tethers, which is affecting the buoyancy of the system (the matrix is response dependent). Hence, the components of the [*K*] matrix are continuously changing at each time step depending upon the response values at the previous time step.

3.3. Mass matrix, [*M*]

The added mass, *M*a, due to the water surrounding the structural members has been considered up to the mean sea level (MSL) and arising from the modified Morison Equation. The presence of off diagonal terms in the mass matrix indicates a contribution of the added mass due to the hydrodynamic loading. The fluctuating components of added mass due to the variable submergence of the structure in water is considered in the force vector depending upon whether the sea surface elevation is above or below the MSL. The added mass matrix of submerged portion of an arbitrarily inclined cylinder can be expressed in terms of the direction cosines. The loading will be attracted only in the surge, heave and pitch degrees of freedom due to the unidirectional wave acting in the surge direction on a symmetric configuration of the platform about the *x* and *z* axes. Therefore, the mass matrix can be written as

$$[M] = \begin{pmatrix} M + M_{a11} & 0 & M_{a13} & 0 & M_{a15} & M_{a16} \\ 0 & M + M_{a22} & M_{a23} & M_{a24} & 0 & M_{a26} \\ M_{a31} & M_{a32} & M + M_{a33} & M_{a34} & M_{a35} & 0 \\ 0 & M_{a42} & M_{a43} & Mr_x^2 + M_{a44} & 0 & 0 \\ M_{a51} & 0 & M_{a53} & 0 & Mr_y^2 + M_{a55} & 0 \\ M_{a61} & M_{a62} & 0 & 0 & 0 & Mr_z^2 + M_{a66} \end{pmatrix} \tag{28}$$

Where, M is the mass of the body, r_x, r_y, and r_z are the radii of gyrations about the *x, y,* and *z*-axes, respectively. For detailed derivation of M_{ij}, see Abou-Rayan l [2009].

3.4. Structural damping [*C*]

The damping matrix [*C*] is calculated by using α and β constants (Rayleigh Damping) as multipliers to the mass matrix [*M*] and stiffness matrix [*K*], respectively.

$$[C]= \alpha[M] + \beta[K] \tag{29}$$

3.5. Hydrodynamic force vector, {*F* (*t*)} on Triangular TLP

The problem of suitable representation of the wave environment is of a prime concern. Once the wave environment is evaluated, wave loading on the structure may be computed based on suitable theory. In this study the water particle position η is determined according to Airy's linear wave theory. Wave and current loading naturally occur simultaneously and current direction may not coincide with wave direction and may vary with depth. The speed may also change with depth. To present a realistic description, a profile which may vary in both magnitude and direction with depth is considered. The current velocity is taken about 10% of wind velocity at a height of 10 m above the water surface. For more details on water particles velocities and accelerations, see Abou-Rayan (2012). For the uni-directional wave train in the surge direction, the force vector {*F* (*t*)}, is given by

$$F(t) = \{F_{11} \quad F_{21} \quad F_{31} \quad F_{41} \quad F_{51} \quad F_{61}\}^T \tag{30}$$

3.6. Solution of the equation of motion in the time domain

The equation of motion is coupled and nonlinear and can be written as

$$[M]\{x^{\bullet\bullet}(t+\Delta t)\} + [C]\{x^{\bullet}(t+\Delta t)\} + [K]\{x(t+\Delta t)\} = \{F\ (t+\Delta t)\} \tag{31}$$

Eq. (31) is nonlinearly coupled, because of the presence of structural displacement, velocity and acceleration in the right hand side of the equation. Therefore, the force vector should be updated at each time step to account for the change in the tether tension. To achieve this response variation a time domain analysis is carried out. The Newmark's beta time integration procedure is used in a step wise manner. It should be

3. RESULTS AND DISCUSSION

A numerical scheme was developed, where solution based on Newmark's beta method was obtained. A major concern was about the effect of the coupling of the degrees of freedom and about its rule in influencing some of the response behaviors critically. Thus, numerical studies for evaluating the coupled and uncoupled responses of the triangular TLP under regular waves have been carried out. Coupling of various degrees-of-freedom was taken into consideration by considering the off-diagonal terms in stiffness matrix [*K*]. On the other hand, these off-diagonal terms were neglected to study the uncoupling effect. Wave forces were taken to be acting in the direction of surge degree-of-freedom. The geometric properties of the TLP and the hydrodynamic

data considered for force evaluation are given in Table 1.

Table 2 shows the coupled and the uncoupled natural time periods and frequencies of the structure. It is seen that natural frequencies in the main soft degrees of freedom (surge, sway, and yaw) are well below the wave frequencies (typical wave spectral peaks are between 0.4 to 1 rad.). Thus, avoiding resonance occurrence and reducing the horizontal motion hence loading on the tether platform system. On the other hand, the other degrees of freedom have higher natural frequencies (above 2 rad.). which means, that all degrees of freedom have frequencies away from the excitation frequency avoiding resonance occurrence.

It is also, noticed that coupling has no effect on the soft degrees of freedom but has some effect on the others specially, the pitch degree of freedom. Therefore, ignoring the coupling effect will lead to overestimation of the pitch response. Time histories of the coupled and the uncoupled responses are shown in Fig.s 7 to 9.

4.1. Surge response

Time histories of surge responses for the triangular TLP are shown in Fig. 7. It is observed that, for a specific wave period, the amplitude of oscillations slightly increases as the wave height increases. Also, the drifting oscillating position increased as the wave height increases. Furthermore, it is inversely proportional to the wave period (i.e. the effect of wave height becomes more pronounced for shorter wave periods). In all cases, the surge response seems to have periodic oscillations that have the same exciting wave period. From response spectrum for surge response, Fig. 12 , it is clear that the motion is periodic with period one for short wave period. The transient state takes about 140-160 seconds for short wave period (6 and 8 sec); whereas it takes about 80 sec for longer wave periods. After that the stationary state begins. Finally, it is observed that coupling has insignificant effect on the surge response. Moreover it is clear that the surge response has no interaction from any degree of freedom. This is attributed to the fact that the loading is in the surge direction.

4.2. Heave response

Time histories of the coupled and the uncoupled heave responses for the triangular TLP are shown in Fig. 8. As expected, the response in the heave direction has very small values compared to that of the surge direction. This is attributed to the relatively high stiffness of the tethers in this direction together with the fact that the excitation is indirect in this case. It is clear that the long wave period causes a more negative heave response offset than that of the short wave periods. Moreover, the heave response is directly proportional to the wave period and to a less extent to wave height. Also, the transient state takes about 40 seconds for short wave periods and about 10 seconds for long wave periods, where the stationary state begins with periodic motion. Which, means that the system tends to stabilizes faster for long wave period (again, effect of the relatively high stiffness of the tethers) . Contribution from surge degree of freedom seems to take place. Finally, coupling seems to have a significant effect on the response for short wave period (6 seconds).

4.3. Pitch response

Time histories of the coupled and the uncoupled pitch responses for triangular TLP are shown in Fig. 9. It is clear that coupling has a significant effect on the pitch

response. This is due to the fact that the structure is not symmetrical in this particular response where two legs exist at the left hand side while only one leg exists at the right hand side. The uncoupled response overestimates the values of the pitch response.It also observed that as the wave period increases the response becomes closer to being periodic in nature. For short wave periods (less than 10 sec.), a higher mode contribution to the response appears to take place. For long wave periods (12.5 and 15 sec.), the higher mode contribution vanishes after one or two cycles and we have a one period response (wave period) as in the surge case. Moreover, the transient state takes about 20 seconds before the stationary state begins. Finally, as the wave period increases, the pitch response decreases. This behavior is more pronounced in the coupled case.

To gain a conceptual view of the stability and periodicity of the dynamic behavior of the structure, the phase plane and the response spectrum for wave height of 8.0 m and wave period of 8 sec. was obtained and the results are shown in Fig. 10. It clear that the steady state behavior of the structure is stable and periodic with period one (multiple harmonics). It should be mentioned that the response spectrum amplitude for surge is extremely high comparing to those of the heave and pitch ones. This is attributed to the fact that the excitation is unidirectional one. Also, response spectrum amplitude of the pitch motion is higher than that of the heave one.

5. CONCLUSIONS

The present study investigates the dynamic response of a Triangular TLP under hydrodynamic forces in the surge direction considering all degrees of freedom of the system. A numerical dynamic model for the TLP was written where Morison's Equation with water particle kinematics using Airy's linear wave theory was used. The scope of the work was to accurately model the TLP system considering added mass coefficients and nonlinearity in the system together with the coupling between various degrees of freedom. Results for the time histories for the affected degrees of freedom have been presented. Based on the results shown in this paper, the following conclusions can be drawn:

- TLP's have very long period of vibration (60 to 100 sec.) associated with motions in the horizontal plane. Since typical wave spectral peaks are between 6 to 15 seconds, resonant response in these degrees of freedom is unlikely to occur.
- While coupling has a non significant effect on the surge, the heave, and tether tension force, it has a significant effect on the pitch response (this is due to the fact that the structure is not symmetric) in which ignoring the coupling effect will lead to overestimation of the pitch response.
- For short wave periods (less than 10 sec), the system responds in small amplitude oscillations about a displaced position that is inversely proportional to the wave period and directly proportional to wave height. On the other hand, for relatively long wave period (12.5 or 15 sec.), the system tends to respond in high oscillations amplitude about its original position. The aforementioned are true for surge and heave responses.
- The heave response is directly proportional to the wave period and to a less extent to wave height and contribution from surge degree of freedom seems to

take place.

- For short wave periods (less than 10 sec.), a higher mode contribution to the pitch response appears to take place. For long wave periods (12.5 and 15 sec.), the higher mode contribution vanishes after one or two cycles and we have a one period response (wave period) as in the surge case.
- For short wave periods (less than 10 sec), the transient state exhibits high tension forces in the tethers. On the other hand, for relatively long wave period (12.5 or 15 sec.), the forces become very smaller and have a mean value of nearly zero.
- The phase plane shows that the steady state behavior of the structure is periodic and stable.
- The pitch response will be highly underestimated if the coupling effect between various degrees-of-freedom is ignored in the analysis of TLP.
- A periodic phenomenon is observed with period one and the structure is stable.

REFERENCES

Abou-Rayan, A.M., Seleemah, A., and, El-gamal, A.R. (2012) "Response of Square Tension Leg Platforms to Hydrodynamic Forces", Ocean Systems Engineering, Vol.2 No.2, pp. 115 – 135.

Bhattachatya, S.K., Anitha, J., Idichandy, V.G. (2004), "Experimental and numerical study of coupled dynamic response of a mini-tension leg platform", Journal of Offshore Mechanics and Arctic, Engineering, 126(4), 318–330.

Chandrasekaran, S. and Roy, A. (2005), "Phase space study of offshore structures subjected to non-linear hydrodynamic loading", Proceedings of the International Conference on Structural Engineering, SEC 2005, Indian Institute of Science, Bangalore.

Chandrasekaran, S., Jain, A. K., Gupta, A., Srivastava, A. (2007a), "Response behaviour of triangular tension leg platforms under impact loading", *Ocean Engineering*, Vol. 34, 45–53.

Chandrasekaran, S., Jain, A. K., Gupta, A. (2007b), "Influence of wave approach angle on TLP's response", Ocean Engineering, Vol. 34, 1322–1327.

Denis. J.P.F. and Heaf, N.J. (1979), "A Comparison between linear and nonlinear response of a proposed Tension Leg Production Platform", Proceedings of the Offshore Technology Conference, OTC 3555, 1743-1754.

Ketabdari, M. J. and Ardakani, H. A. (2005), "Nonlinear response analysis of a sea star offshore tension leg platform in six degrees of freedom", *WIT Transactions on the Built Environment 84.*

Kurian, V.J., Gasim, M.A., Narayanan, S.P., Kalaikumar, V. (2008a), "Parametric Study of TLPs Subjected to Random Waves", *ICCBT-C-19*, 213-222.

Kurian, V.J., Gasim, M.A., Narayanan, S.P., Kalaikumar, V. (2008b), "Response of Square and Triangular TLPs Subjected to Random Waves", *ICCBT-C-12*, 133-140.

Lee, H.H. and Wang, P. W. (2000), "Analytical solution on the surge motion of tension leg twin platform structural systems", *Ocean Engineering,* Vol. 27, 393–415.

Low, Y. M. (2009), "Frequency domain analysis of a tension leg platform with statistical linearization of the tendon restoring forces", *Marine Structures,* Vol. 22, 480–503.

Yang, C. K. and Kim, M. H., (2010), "Transient effects of tendon disconnection of a TLP by hull–tendon–riser coupled Dynamic analysis", *Ocean Engineering*, Vol. 37, 667–677.

Table 1. Geometric properties of the triangular TLP and load data

Water properties		Platform properties			
Gravity acceleration (m/sec^2)	9.81	Platform weight (KN),W	280000	Center of gravity above the sea level (m), H_C	6.03
Water weight density (kN/m^3)	10.06	Platform length (m), Pl	66.22	Tether stiffness (KN/m),γ	80000
Inertia coefficient, C_m	2			Tether length (m), L	569
Drag coefficient, C_d	1	Platform radius of gyration in x-directions (m), r_x	32.1	Platform radius of gyration in y-directions (m), r_y	32.1
Current velocity (m/sec),U_c	0	Platform radius of gyration in z-directions (m), r_z	33	Water depth (m),d	600
Wave period (sec), T_w	6,8,10, 12.5 and 15	Tether total force (KN),T	160000	Diameter of pontoon (m), D_P	11
Wave height (m), H_w	8, 10 and 12	Diameter of columns (m), D_c	20	Draft(m),D_r	31
				Damping ratio, ζ	5%

Table 2. Natural structural frequencies (*f in rad./sec*.) and periods (*T in sec.).*

Analysis Case	DOF											
	Surge		Sway		Heave		Roll		Pitch		Yaw	
f/T	*f*	*T*	*f*	*T*	*f*	*T*	*f*	*T*	*f*	*T*	*f*	*T*
Coupled	0.064	97.245	0.064	97.254	2.522	2.491	2.095	2.997	2.058	3.052	1.001	62.729
Uncoupled	0.064	97.205	0.064	97.205	2.487	2.526	1.860	3.377	1.853	3.389	0.099	62.969

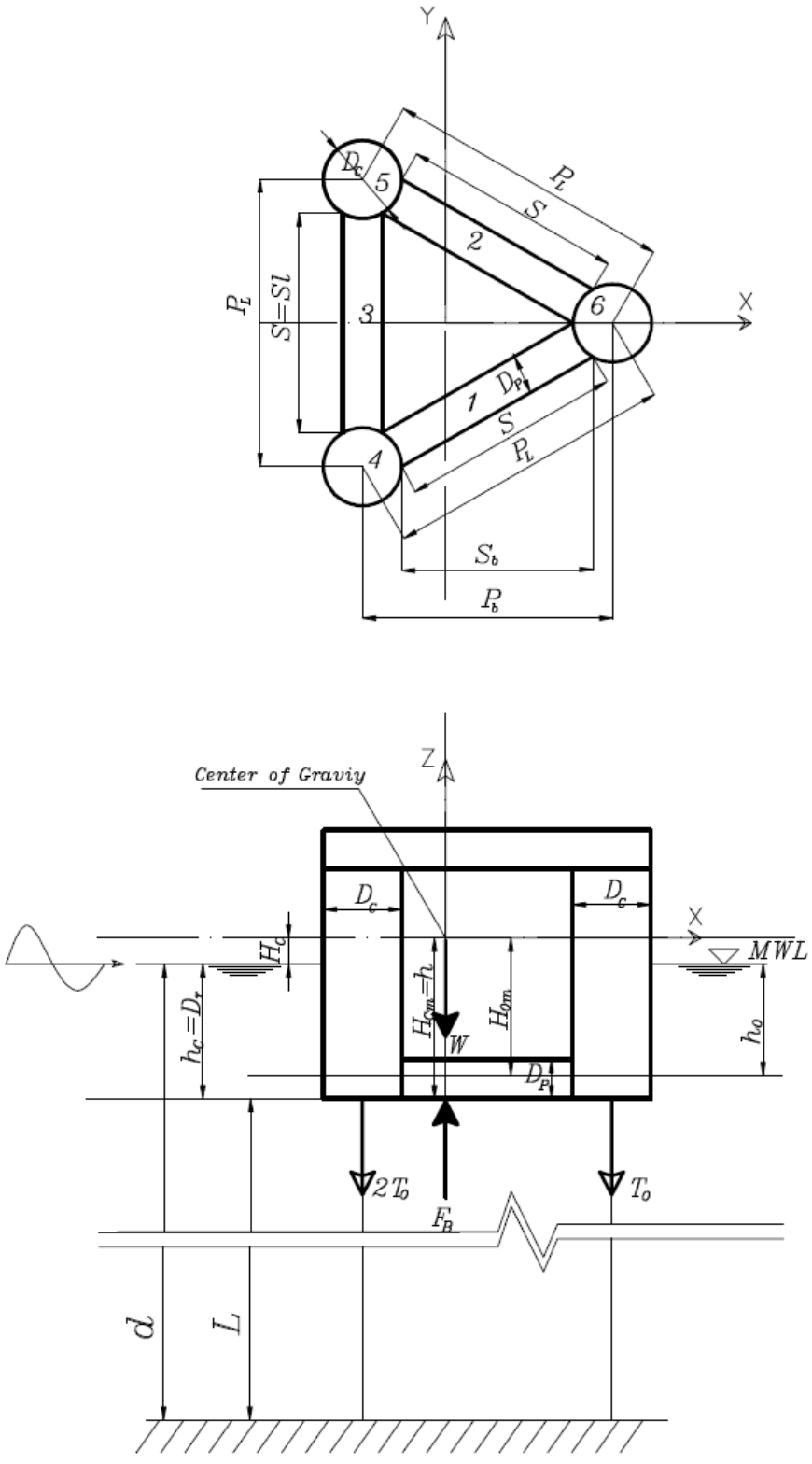

Fig. 1. The Triangular TLP (plan and elevation).

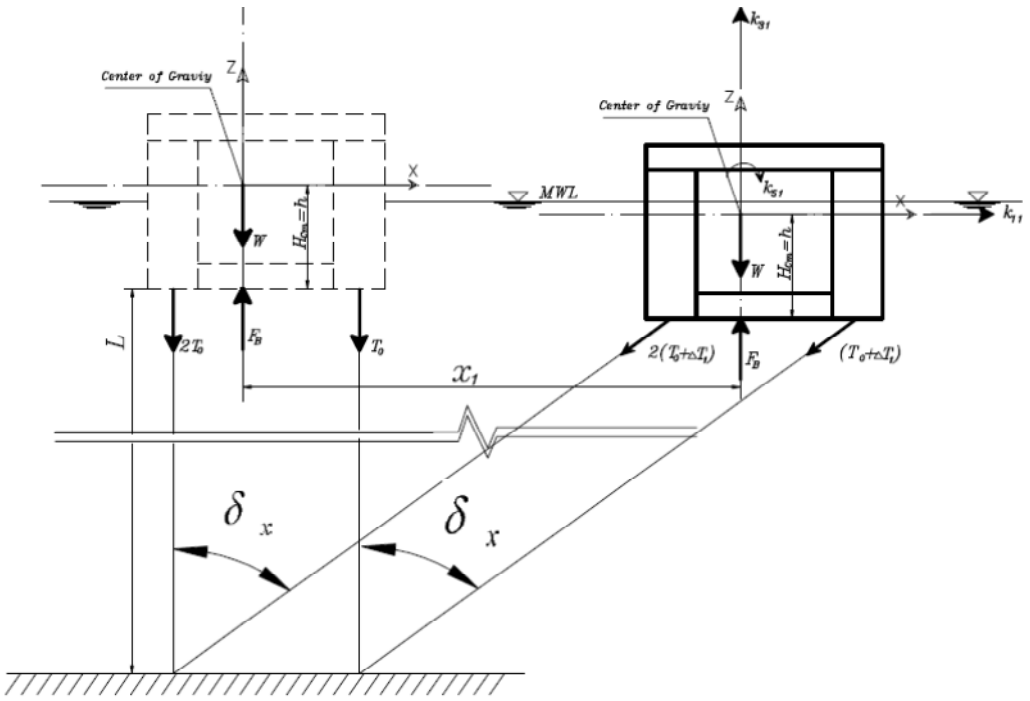

Fig. 2. The Surge displacement in a triangular TLP.

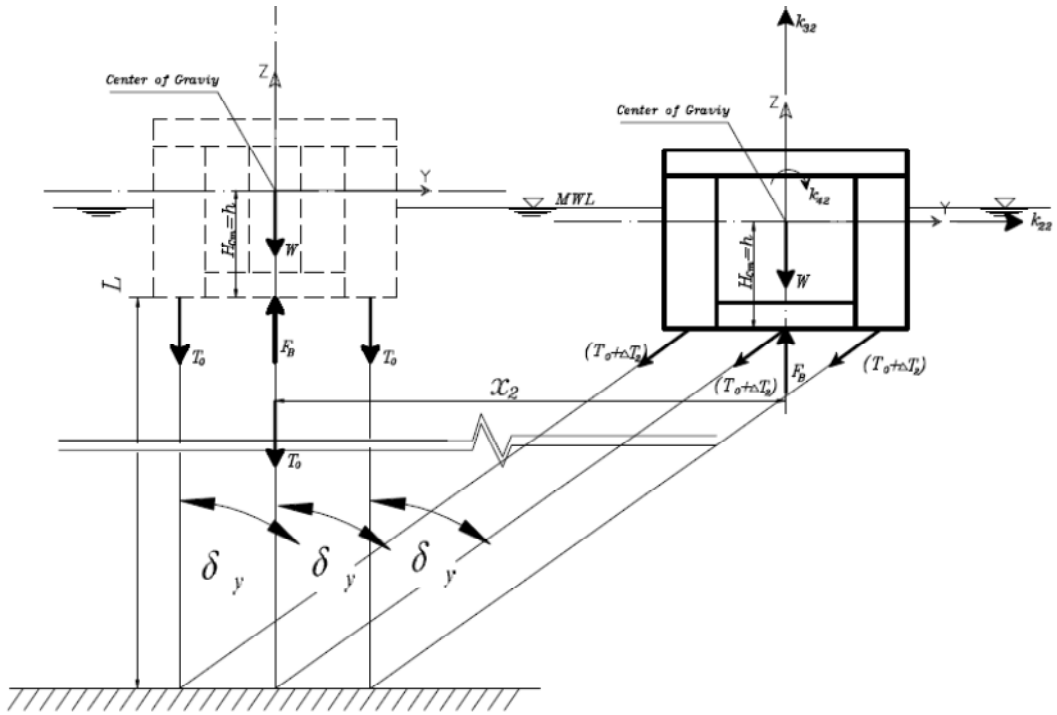

Fig. 3. The Sway displacement in a triangular TLP

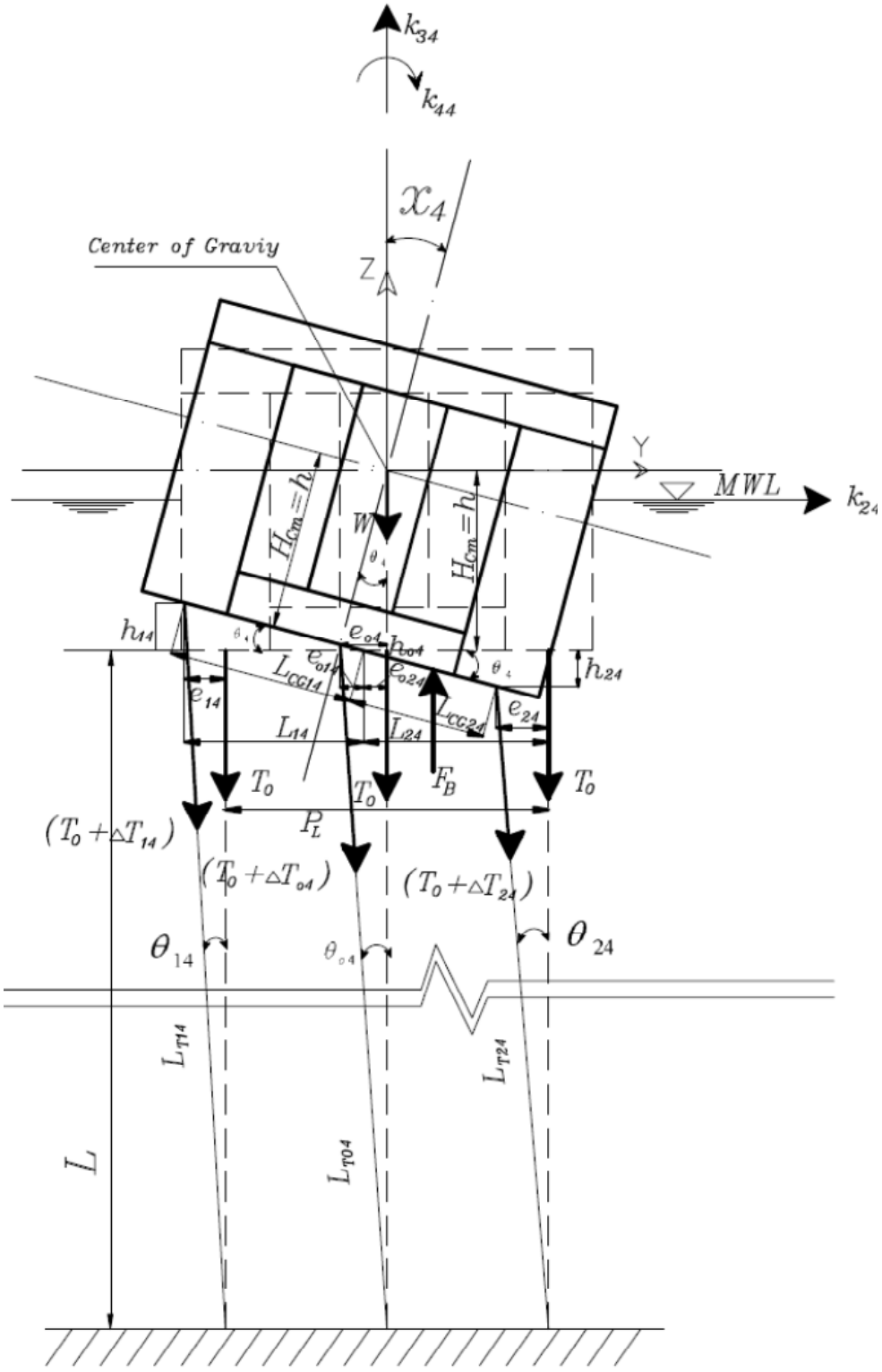

Fig. 4. The Roll displacement in a triangular TLP.

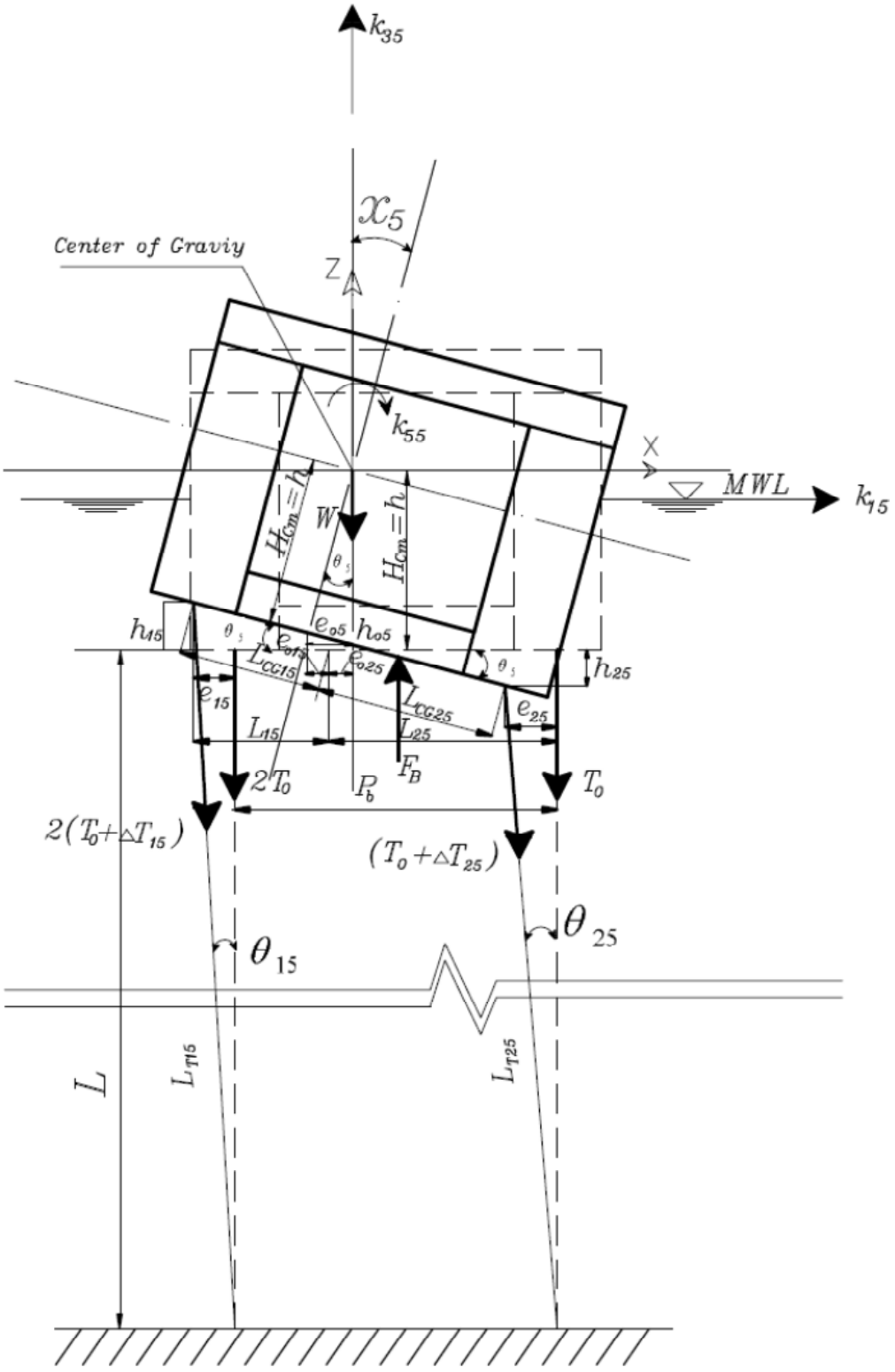

Fig. 5. The Pitch displacement in a triangular TLP.

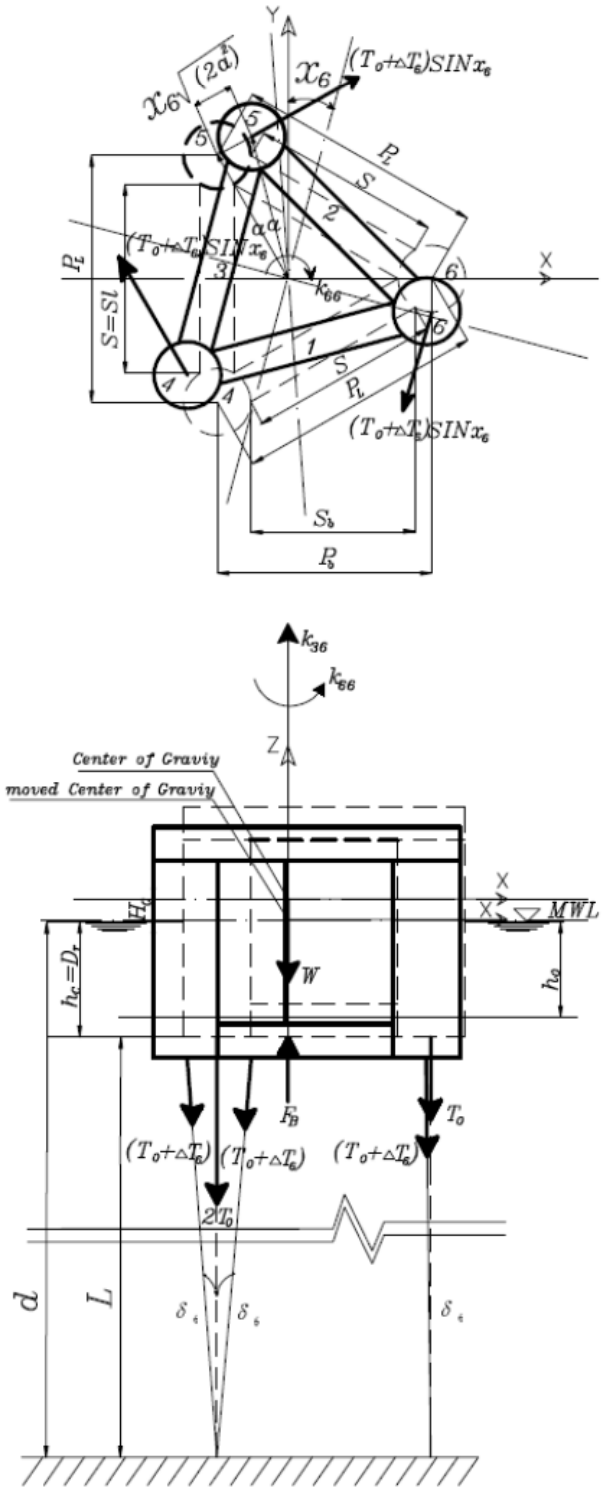

Fig. 6. The Yaw displacement in a triangular TLP.

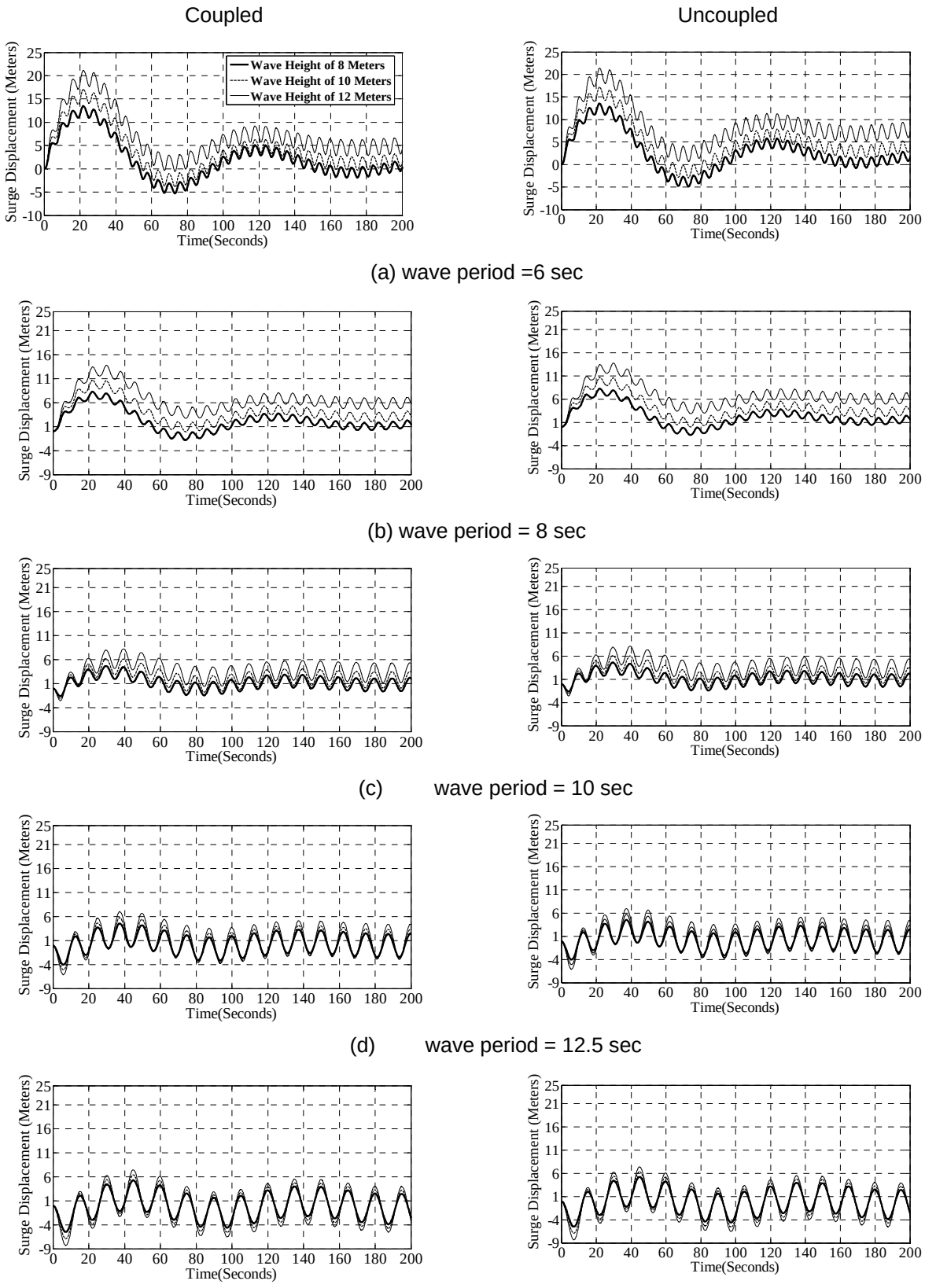

(a) wave period =6 sec

(b) wave period = 8 sec

(c) wave period = 10 sec

(d) wave period = 12.5 sec

(e) wave period = 15 sec

Fig. 7. Surge response of triangular TLP

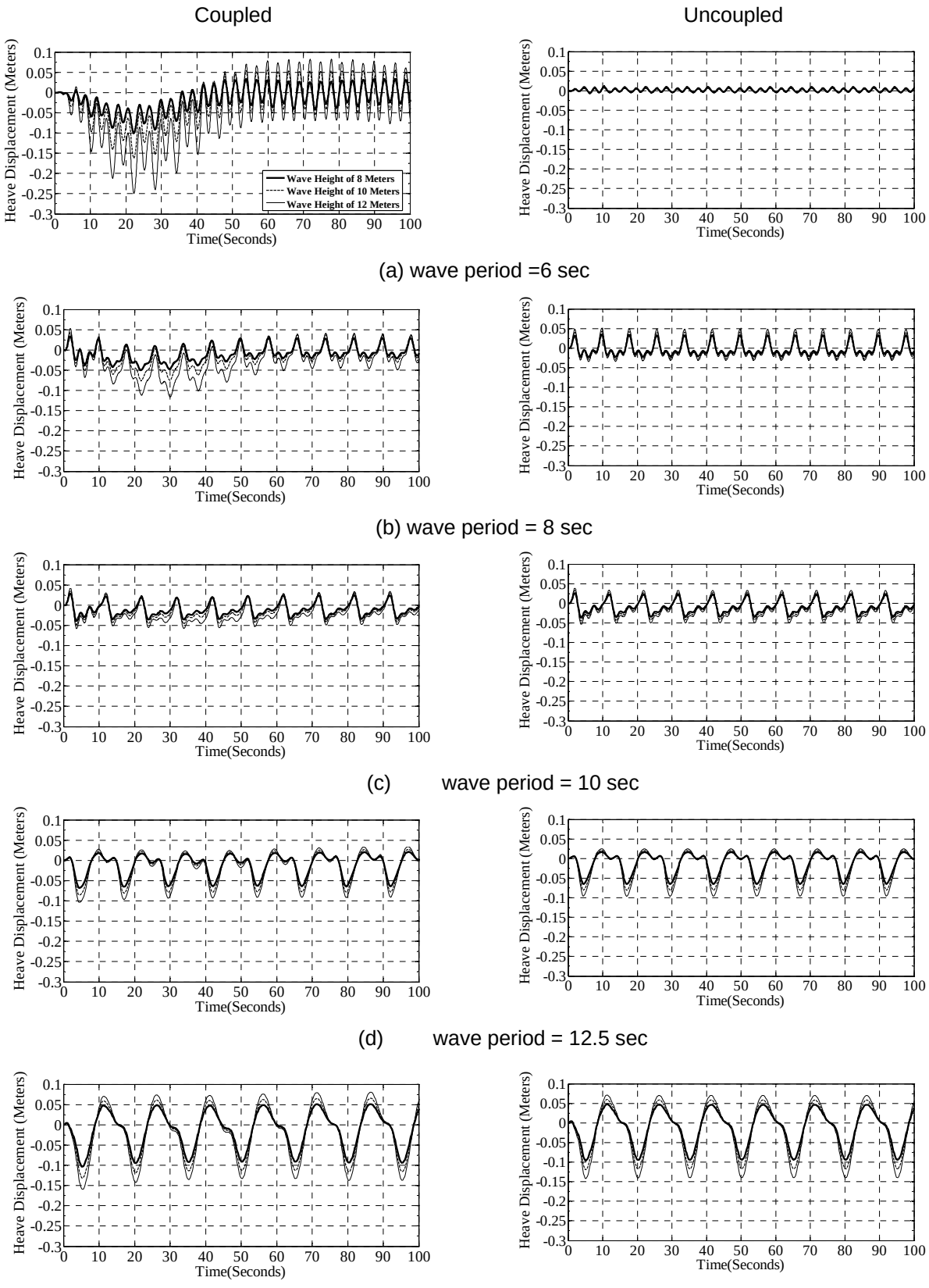

(a) wave period =6 sec

(b) wave period = 8 sec

(c) wave period = 10 sec

(d) wave period = 12.5 sec

(e) wave period = 15 sec

Fig. 8. Heave response of square TLP

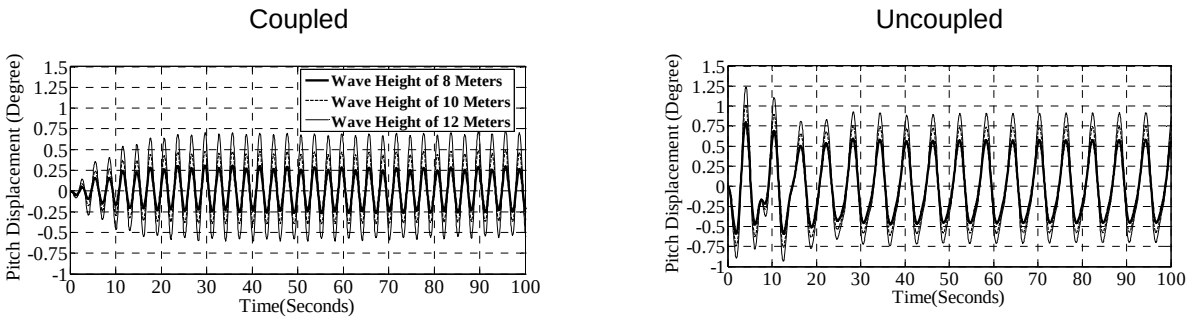

(a) wave period =6 sec

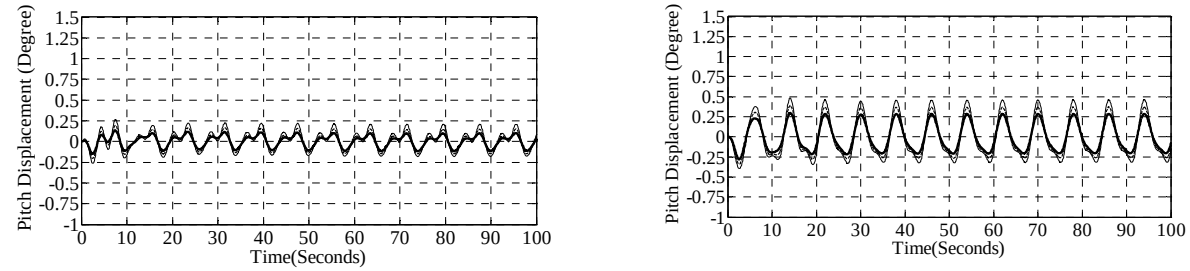

(b) wave period = 8 sec

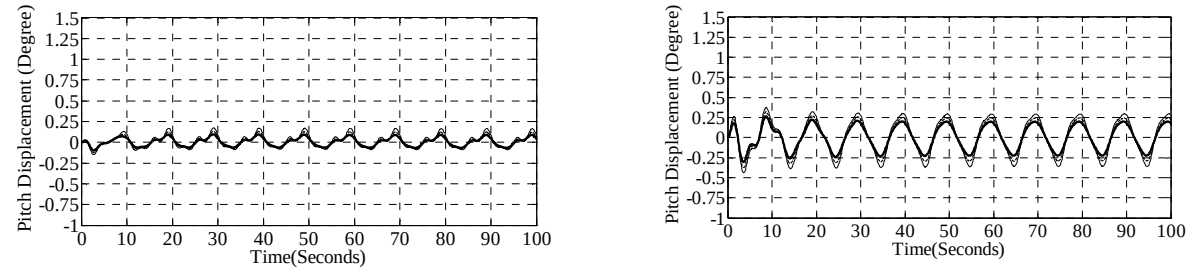

(c) wave period = 10 sec

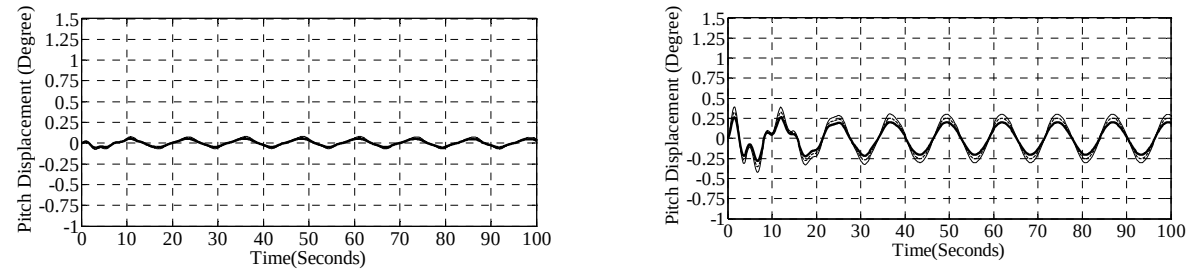

(d) wave period = 12.5 sec

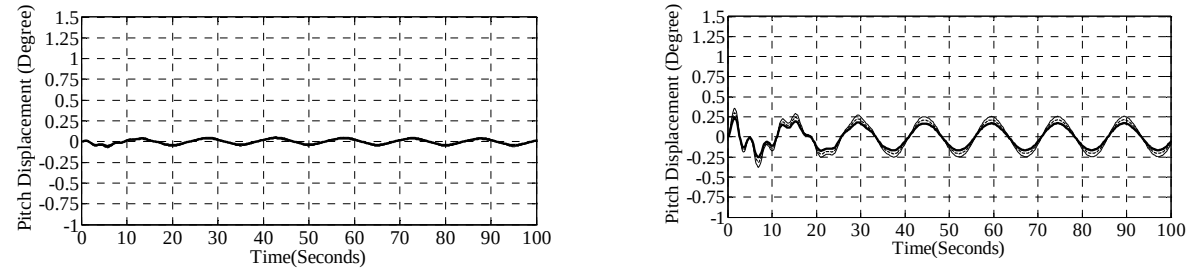

(e) wave period = 15 sec

Fig. 9. Pitch response of square TLP

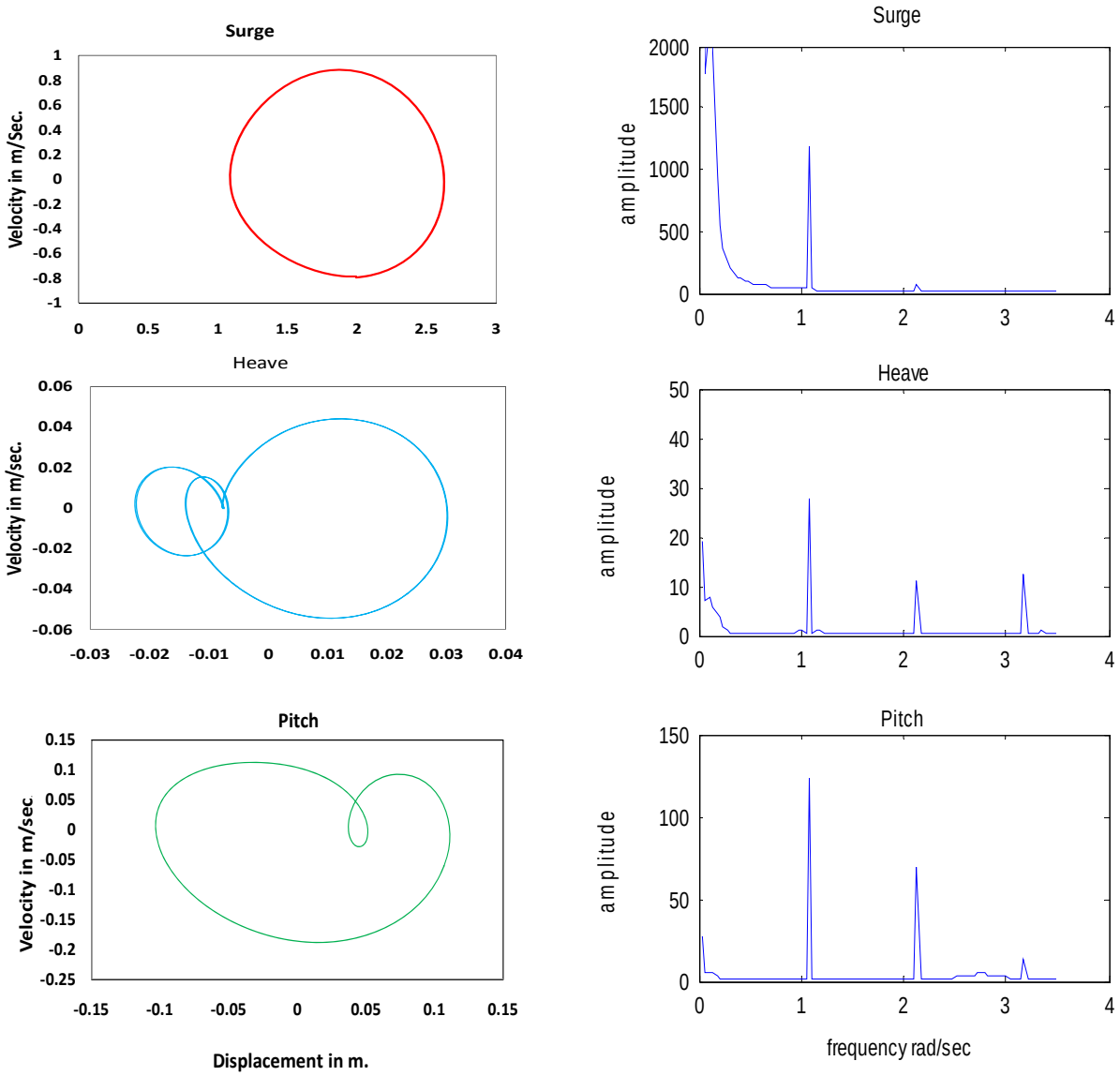

Fig. 10. Phase plane and response spectrum for wave period= 8 sec. and height = 8.0m.